Reviving oncogenic addiction to MET bypassed by BRAF (G469A) mutation

Anna Rita Virzì[a,1], Alessandra Gentile[a,1,2], Silvia Benvenuti[a], and Paolo M. Comoglio[a]

[a]Laboratory of Molecular Therapeutics and Exploratory Research, Candiolo Cancer Institute, Fondazione del Piemonte per l'Oncologia- Istituto di Ricovero e Cura a Carattere Scientifico (FPO-IRCCS), 10060 Candiolo, Italy

Cancer clonal evolution is based on accrual of driving genetic alterations that are expected to cooperate and progressively increase malignancy. Little is known on whether any genetic alteration can hinder the oncogenic function of a coexisting alteration, so that therapeutic targeting of the one can, paradoxically, revive the function of the other. We report the case of a driver oncogene (MET) that is not only bypassed, but also disabled by the mutation of a downstream transducer (BRAF), and reignited by inhibition of the latter. In a metastasis originated from a cancer of unknown primary (CUP), the MET oncogene was amplified eightfold, but unexpectedly, the kinase was dephosphorylated and inactive. As result, specific drugs targeting MET (JNJ-38877605) failed to inhibit growth of xenografts derived from the patient. In addition to MET amplification, the patient harbored, as sole proliferative driver, a mutation hyperactivating BRAF (G469A). Surprisingly, specific blockade of the BRAF pathway was equally ineffective, and it was accompanied by rephosphorylation of the amplified MET oncoprotein and by revived addiction to MET. Mechanistically, MET inactivation in the context of the BRAF-activating mutation is driven through a negative feedback loop involving inactivation of PP2A phosphatase, which in turn leads to phosphorylation on MET inhibitory Ser985. Disruption of this feedback loop allows PP2A reactivation, removing the inhibitory phosphorylation from Ser985 and thereby unleashing MET kinase activity. Evidence is provided for a mechanism of therapeutic resistance to single-oncoprotein targeting, based on reactivation of a genetic alteration functionally dormant in targeted cancer cells.

MET amplification | BRAF | MET target therapy

Cancers evolve by a reiterative process of clonal expansion, genetic diversification, and clonal selection in which the tissue provides the context for cancer cell evolution. Cancer can be considered as an ecosystem continuously adapting to changing environments, where the driving force is represented by intrinsic mutability of cancer cells, following the rules of Darwinian evolution (1, 2). The competition for space and resources allows colonization of other organs, giving rise to distant metastases.

Little is known about how multiple alterations coexist in the same cancer lesion. In some cases, an early genetic alteration is taken over by a new one impinging on the same molecular pathway, usually at the downstream level, thereby bypassing the early mutation. The late mutation confers resistance to therapy targeting the early mutation, but renders cancer cells sensitive to specific inhibitors of the latter (3).

The role of aberrant activation of the MET oncogene in driving the malignant progression and metastasization has been widely documented (4, 5). MET is genetically altered at uncommonly high frequency in cancers of unknown primary site (CUP) (6), a mysterious, lethal clinical entity, featuring multiple metastases in the absence of a detectable primary tumor. Constitutive MET activation occurs through several mechanisms including gene amplification, activating genetic mutations, transcriptional up-regulation, or ligand-dependent autocrine or paracrine mechanisms (7). Activated MET receptors propagate an intricate system of signaling cascades leading to the

acquisition of cell motility, proliferation, and escape from apoptosis. Taken together, these biological events recapitulate a biological program defined as invasive growth (8). The versatility of MET-mediated biological responses is sustained by qualitative (i.e., engagement of dedicated signal transducers) and quantitative [i.e., either recruitment of adaptor amplifiers or desensitization through internalization, degradation (9) or negative feedback by phosphorylation of regulatory residues (10, 11)] signal modulation. A number of MET kinase inhibitors have been developed over the last 10 y and are currently in clinical trials (5). In cancer cell lines or patient-derived tumor xenografts, it has been shown that only tumors displaying MET genetic lesions (mostly amplification) respond to MET blockade with apoptosis and/or cell cycle arrest in vitro (12) and tumor growth inhibition in vivo (13). Similar to the case of oncogenic kinase receptor, resistance to targeting drugs occurs and is mediated by aberrant activation of other downstream signal transducers (14, 15).

MET-dependent signals are organized in pathways that are shared among different tyrosine kinase receptors, including the MAPK cascade (RAS-RAF-MEK-ERK). The BRAF Ser/Thr kinase (16) is mutated in ∼50% of melanomas and in ∼8% of all cancer (17), with almost all mutations falling in the kinase domain (18, 19). The most common mutation encodes the constitutively active BRAF-V600E oncoprotein, specifically targeted by vemurafenib (20). Despite the initial success of this and other BRAF inhibitors, drug resistance is invariably observed (21). Resistance is mostly a result of reactivation of the MAPK pathway that occurs through stromal extracellular or cell-autonomous survival signals mediated by tyrosine kinase

Significance

Genetic alterations of two oncogenes occur frequently in cancers; however, silencing of an oncogenic driver by activation of a second oncogene has never been described. Here we report the case of a cancer carrying alterations of two oncogenes residing on the same pathway; namely, MET amplification and BRAF mutation. Surprisingly, the pharmacological blockade of BRAF had no effect, as it was followed by MET reactivation: Mechanistic studies unraveled the existence of a previously unknown negative feedback inhibition of MET by BRAF. This phenomenon provides evidence for a mechanism of resistance to therapy against a single-target oncogene.
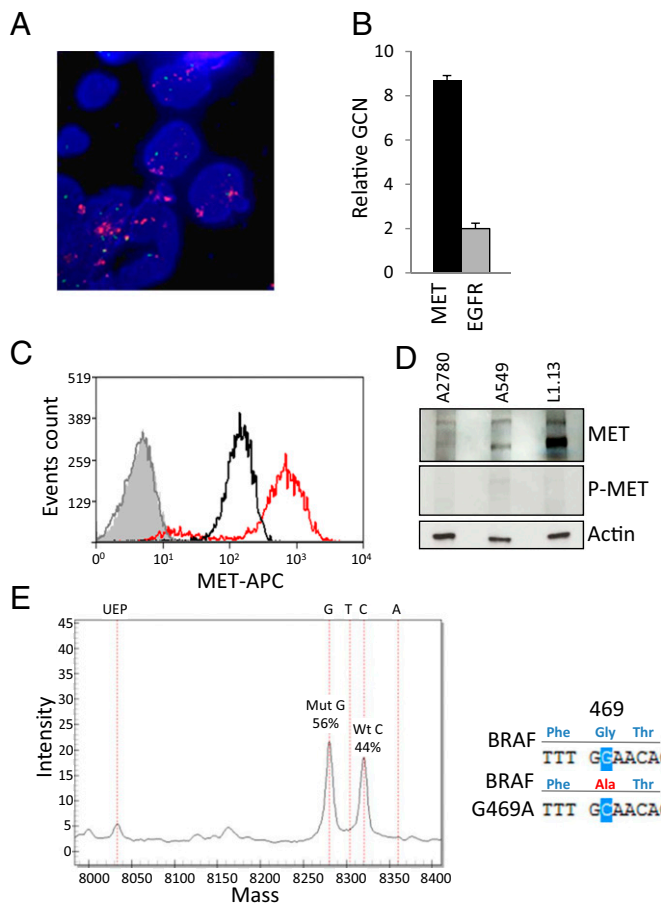
Fig. 1. Concomitant amplification of MET and mutation of BRAF in a liver metastasis. A bioptic fragment, harvested from a 64-y-old patient affected by a CUP1.13, was s.c. implanted in an immunocompromised NOD/SCID mouse to obtain PDX1.13. All biological and genetic features of the original tumor were maintained in PDX and in a derived cell line (L1.13). (*A*) FISH analysis on FFPE samples obtained from the patient was performed with probes specific for MET (red) and Chr.7 centromere (green). The picture shows multiple red signals resulting from gene amplification (MET mean copy number: 17.6; Centromere 7 mean copy number: 2.05; MET/CEP 7 Ratio 8.6). (*B*) Gene copy number (GCN) was determined by RT-PCR on genomic DNA extracted from PDX tumor. The number of MET (black) and EGFR (gray) copies were determined using diploid A549 cells as reference (https://cancer. sanger.ac.uk/cell_lines). To exclude the polysomy of the entire Chr.7, the EGFR gene, located on the same arm of the Chr.7, was evaluated. (*C*) Flow cytometric analysis of MET expression at the cell surface of the L1.13 cell line (red), compared with a MET negative cell line (A2780, gray) and a cell line expressing normal level of MET (A549, black). Photomultiplier tube (PMT) voltages were set using an unstained sample of L1.13 (fill gray). (*D*) Western blot analysis of lysates from A2780, A549, and L1.13 cells. Despite its overexpression in L1.13, MET is not Tyr-phosphorylated. Actin was used as loading control. (*E*) Genomic analysis of CUP1.13 by OncoCarta interrogating 238 mutations across 19 oncogenes (SEQUENOM OncoCarta Assay Panel v1.0), revealed a BRAF missense mutation (c.1406G, enlighten on the *Right*) falling in exon 11, encoding the kinase domain. (*Left*) MassARRAY analysis. The expected positions for the unextended primer (UEP), and the extension products (mutant and WT) are indicated. The proportion of peak areas and the specific base are also shown.

receptors such as AXL (22) or MET (23, 24). MEK inhibitors display clinical efficacy to overcome resistance to BRAF blockade (25–27).

Here we identified and characterized a molecular mechanism of resistance in a CUP tumor harboring two concomitant mutations affecting MET and BRAF. In this tumor, inhibition of either oncogene was ineffective because of reactivation of MET

quenched by a previously unknown mechanism of negative feedback by BRAF. These findings unravel the existence of a mechanism of resistance to target monotherapy.
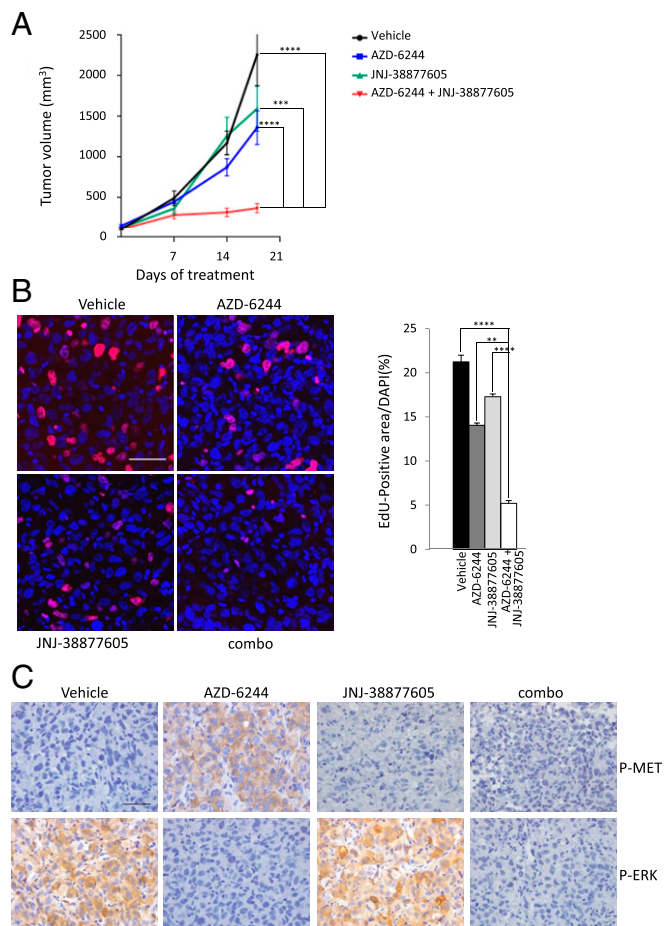

Fig. 2. Inhibition of the BRAF pathway restores sensitivity to MET inhibitor in vivo. (*A*) Tumor growth curves of PDX1.13 established as earlier, passed on and randomized to obtain the same volume average (250–300 mm^3) and distributed in four cohorts consisting of six mice. PDXs were treated daily for 18 d with vehicle (black line), AZD-6244 (blue line), JNJ-33877605 (green line), or their combination (red line). Tumor size was evaluated weekly. Each symbol represents the average tumor volume at the indicated time ± SEM. Bars represent the SD. By two-way ANOVA analysis, $P = 0.0005$ (AZD-6244 + JNJ-33877605 vs. AZD-6244), $P < 0.0001$ (AZD-6244 + JNJ-33877605 vs. JNJ-33877605), and $P < 0.0001$ (AZD-6244 + JNJ-33877605 vs. vehicle). Treatment with either MEK or MET inhibitors failed to significantly inhibit tumor growth, whereas the combination of the two drugs elicited growth arrest. (*B*) Detection of cells entering the S-phase of the cycle by incorporation of the thymidine analog 5-ethynyl-2′-deoxyuridine (EdU: red). The percentage of cells entering the S-phase was estimated by EdU i.p. injections 24 h before death. (*B*, *Left*) Representative merged confocal images of FFPE samples of PDX1.13 tumors untreated (vehicle) or treated with AZD-6244, JNJ-38877605, or the combination of the two. (Scale bar: 50 μm.) (*B*, *Right*) Quantitative analysis of EdU-positive cells present in areas normalized for DAPI staining (blue in the *Left*). In the graph, the black bar indicates vehicle treatment, the dark gray bar AZD-6244, the gray bar JNJ-33877605, and the white bar the combination of AZD-6244 and JNJ-33877605 (means ± SEM; 15 fields/tumor were quantified). $P = 0.001743898$ (AZD-6244+ JNJ-33877605 vs. AZD-6244), $P < 0.0001$ (AZD-6244 + JNJ-33877605 vs. JNJ-33877605), and $P < 0.0001$ (AZD-6244 + JNJ-33877605 vs. vehicle), Student's *t*-test. (*C*) Phosphorylation of MET and ERK in FFPE slides obtained from PDX1.13 tumors, untreated (vehicle) or treated with the indicated drugs. Immunohistochemistry (IHC) analysis was performed by MET phospho-tyrosine (P-MET) or phospho-threonine/tyrosine (P-ERK) antibodies. MET is phosphorylated only on AZD-6244 treatment. ERK is not phosphorylated in the presence of AZD-6244. Combined treatment with AZD-6244 and JNJ-38877605 abrogates phosphorylation of both MET and ERK. (Scale bar: 50 μm.) **$P < 0.01$; ***$P < 0.001$; ****$P < 0.0001$.
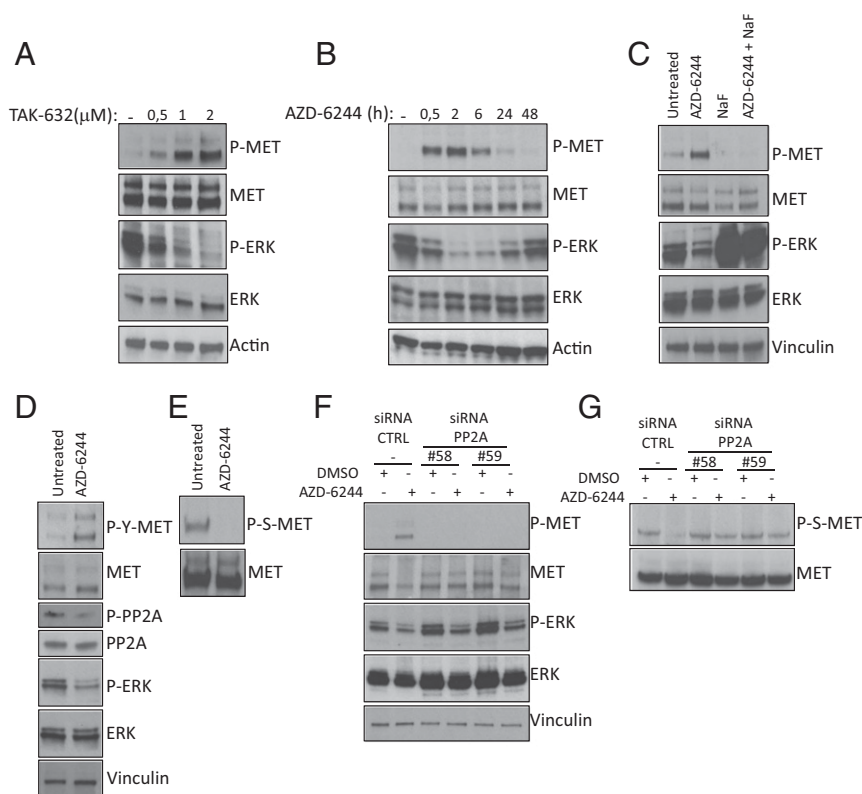
CELL BIOLOGY

Fig. 3. Mechanistic explanation of the feedback loop between BRAF and MET. Biochemical analysis of phosphoproteins from L1.13 cell lysates treated with different inhibitors and analyzed by immunoblotting. (*A*) Treatment with increasing concentrations of TAK-632. The BRAF specific inhibitor induces dose–response MET phosphorylation, whereas P-ERK coherently decreases. (*B*) Time-course treatment of L1.13 cells with AZD-6244 (500 nM). MEK inhibition recapitulates BRAF inhibition and is followed by MET phosphorylation. (*C*) Treatment of L1.13 cells for 30 min with the Ser/Thr phosphatases inhibitor sodium fluoride, NaF (25 mM), alone or in combination with AZD-6244 (500 nM). NaF abrogates AZD-6244-induced MET phosphorylation, indicating the involvement of a Ser/Thr phosphatase in the phenomenon. (*D* and *E*) Treatment of L1.13 with AZD-6244 500 nM for 30 min is followed by concomitant activating dephosphorylation of PP2A phosphatase, MET Ser985 dephosphorylation (immunoprecipitates in *E*). (*F* and *G*) Silencing of PP2A Ser/Thr phosphatase by two siRNAs (#58 and #59) targeting different sites. Scrambled siRNA was used as control (CTRL). Cells were treated with AZD-6244 (500 nM) for 30 min, and lysates were analyzed as earlier. DMSO was used as control vehicle. PP2A silencing prevents AZD-6244-induced MET Tyr1234-1235 phosphorylation (*F*) and abrogates dephosphorylation of MET Ser985 (immunoprecipitates in *G*). Antibodies used for Western blots analysis: P-Y/S-MET, MET antibody recognizing Tyr1234-1235 and Ser985 in the phosphorylated state, respectively. MET, antibody against the MET β chain; P-ERK, antibody against phosphorylated ERK; ERK, antibody against the ERK protein. Vinculin or actin antibodies have been used to normalize the amount of loaded proteins.

Results and Discussion

We here report a tumor that concomitantly harbors an amplification of the MET oncogene and an activating mutation in BRAF. This tumor was a liver metastasis of a CUP. Although we cannot chart the evolutionary trajectory of this case (CUP1.13), it is likely that the mutation in BRAF, a downstream MET signal transducer (28), occurred as a stochastic secondary event after the acquisition of MET gene amplification. This is reminiscent of the sequence of mutations emerging when tumor genetic evolution is driven by the selective pressure of targeted inhibitors such as HER-2 inhibitory antibodies in breast cancer (29, 30) or BRAF inhibitors in melanoma (31), which cause the emergence of genetic alterations in the downstream effectors PI3K/PTEN or MEK, respectively. Here we report that, unexpectedly, the mutation affecting BRAF bypasses MET amplification, but it does not engender sensitivity to specific BRAF inhibitors. We found that this is the result of a so-far-unrecognized negative feedback loop between BRAF and MET, in which the BRAF pathway quenches MET activity, impinging on the negative regulatory Ser985 located in the juxtamembrane domain (11). As result, BRAF inhibition unleashes phosphorylation of amplified MET (4, 5). Ligand-independent activation of the MET kinase by amplification and overexpression has been established in a wide spectrum of tumors (for a review, see ref. 7).

In CUP1.13, MET was eightfold amplified (Fig. 1 *A* and *B*), overexpressed and exposed at the cell surface (Fig. 1*C*), but unexpectedly silent (Fig. 1*D*). MET amplification was combined to a second uncommon downstream oncogenic mutation, G469A, affecting BRAF (Fig. 1*E*) (17). Next-generation analysis of a panel of 241 cancer-related genes detected only one additional mutation, SMO R726Q (*SI Appendix*, Table S1). Following these observations, patient-derived xenografts (PDXs) carrying the CUP1.13 tumor (CUP1.13 PDXs) were treated with the specific MET inhibitor JNJ-38877605 (15), which was ineffective, as expected (Fig. 2*A*). PDXs were then treated with the MEK inhibitor AZD-6244 (32), acting downstream of BRAF, as a result of the lack of specific direct inhibitors manageable for in vivo treatment. Nevertheless, inhibition of BRAF pathway was ineffective as well (Fig. 2*A*). However, concomitant treatment with the two drugs inhibiting MET and MEK significantly impaired tumor growth (Fig. 2*A*). These data were strengthened by measuring the percentage of cells entering S-phase by incorporation of the thymidine analog 5-ethynyl-2′-deoxyuridine (Fig. 2*B*). Immunohistochemical staining of paraffin-embedded PDX tumor slides showed that treatment with AZD-6244 significantly quenched phosphorylation of the MEK substrate ERK, while unexpectedly restoring Tyr-phosphorylation of the MET receptor (Fig. 2*C*). These data were confirmed by biochemical experiments performed on a cell line derived from
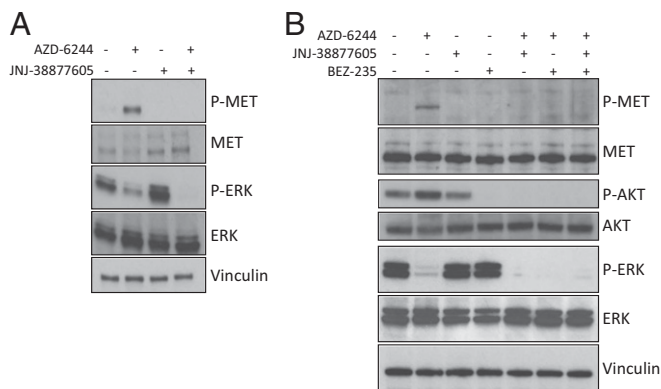
Fig. 4. MET and BRAF inhibition. Immunoblotting analysis of phosphoproteins from L1.13 cells treated with MET and/or MEK inhibitors and/or PI3K-mTOR inhibitor. (*A*) Treatment with AZD-6244 (500 nM) and JNJ-33877605 (250 nM) alone or in combination for 30 min. AZD-6244 treatment is followed by MET phosphorylation. ERK is fully dephosphorylated on concomitant treatment with MET and MEK inhibitors. The increase of ERK phosphorylation after treatment with JNJ-38877605 is unexpected and possibly related to the adverse effect of the drug. (*B*) Treatment with AZD-6244 (500 nM), JNJ-33877605 (250 nM) and BEZ-235 (250 nM) alone or in combination for 30 min. AZD-6244 treatment induces MET phosphorylation. AKT activity increases when MEK is inhibited. ERK is fully dephosphorylated when the cells are treated with MEK inhibitor in combination with PI3K-mTOR inhibitor or MET inhibitor.

CUP1.13 PDX (L1.13). TAK-632 (33), a specific BRAF inhibitor suitable for in vitro experiments, or AZD-6244, inhibiting MEK in the downstream pathway, restored MET Tyr-phosphorylation (Fig. 3 *A* and *B*). These observations unveil a previously unrecognized negative feedback loop between MET and the BRAF pathway. This loop, fixed in cancer cells harboring an activating mutation of BRAF, may operate in physiological conditions as well, providing a mechanism to restrict MET signaling in time. A similar regulatory feedback loop operates in the case of epithelial growth factor receptor (EGFR) (34). To check the specificity of the loop in L1.13 overexpressing MET, we screened 49 tyrosine kinase receptors by antibody-based phosphoproteomics. In these cells, other than a slight effect on EGFR, MEK inhibition unbridles kinase activity of MET specifically (*SI Appendix*, Fig. S1). To get insight in the mechanism underlying this phenomenon, we considered the relatively fast kinetics (peak of MET phosphorylation at 30 min, plateau at 2 h, and drop from 6 h on; Fig. 3*B*) and focused on posttranslational mechanisms. The kinetics suggest the involvement of activation/inactivation of Ser/Thr phosphatases/kinases that regulate MET kinase activity. Treatment with sodium fluoride, a selective Ser/Thr phosphatase inhibitor (35), completely inhibited rephosphorylation of MET in the presence of MEK inhibitor (Fig. 3*C*). We thus focused on the Ser/Thr phosphatase PP2A, known to dephosphorylate MET at Ser985 (36). We previously showed that MET phosphorylation on the regulatory Ser985 represents the major regulatory site responsible for MET kinase inhibition (11). Treatment of L1.13 cells with AZD-6244 decreased PP2A phosphorylation on Tyr307 (Fig. 3*D*). This is known to trigger phosphatase activity of PP2A (37) and was found to reduce MET Ser985 phosphorylation (Fig. 3*E*), and to activate MET kinase (Fig. 3*E*). Moreover, in a separate experiment, two specific PP2A siRNAs completely inhibited the feedback loop and fully prevented MET rephosphorylation in the catalytic domain by impairing dephosphorylation of the Ser985 (Fig. 3 *F* and *G* and *SI Appendix*, Fig. S2). This finding is in agreement with phosphoproteomic studies showing that AZD-6244 downmodulates MET Ser985 phosphorylation (38).

In L1.13 cells, ERK phosphorylation was strongly decreased by treatment with AZD-6244, but not completely lost (Fig. 3 *A*–

C). Full inhibition was, however, observed after concomitant treatment with the MET inhibitor JNJ-38877605 (Fig. 4*A*). This observation suggests that, given the branching nature of the signaling network emanating from MET (39), the residual ERK activity after MEK inhibition is driven through an alternative pathway, such as the PI3K pathway (40). Accordingly, blockade of PI3K in L1.13 cells, where MET was reactivated by the MEK inhibitor, completely abrogated ERK activity (Fig. 4*B*), supporting the involvement of the MET/PI3K/AKT axis.

Taken together, these data provide the mechanistic explanation for the negative feedback loop between BRAF and MET in this cancer cell line, via inactivation of the phosphatase PP2A (Fig. 5). Even if other mechanisms may be envisaged, the circuit involving BRAF/MEK and PP2A is necessary and sufficient for the feedback of MET inhibition.

It is an accepted notion that tumors are composed by genetically heterogeneous subclones, some of which rise while others shrivel to deal with stromal selective pressure (41, 42). A subclone harboring an early oncogenic mutation may develop a later mutation more effective in promoting adaptation and the emergence of a progeny endowed with increased malignancy. If the late mutation impinges on the same signaling pathway, its targeting should be, in principle, effective. The data reported here unveil and explain a paradox of targeted therapy: quenching the effects of a late mutation restores sensitivity to drugs targeting what it is likely to be an earlier mutation. We show that, in the case of MET and BRAF oncogenes, the paradox is generated by an inhibitory feedback loop, mediated by a protein serine phosphatase. The key role of phosphatases as negative regulators of signal transduction has been already observed in the case of other tyrosine kinase receptors (43). At first sight, it is counterintuitive, considering treating a patient featuring a BRAF
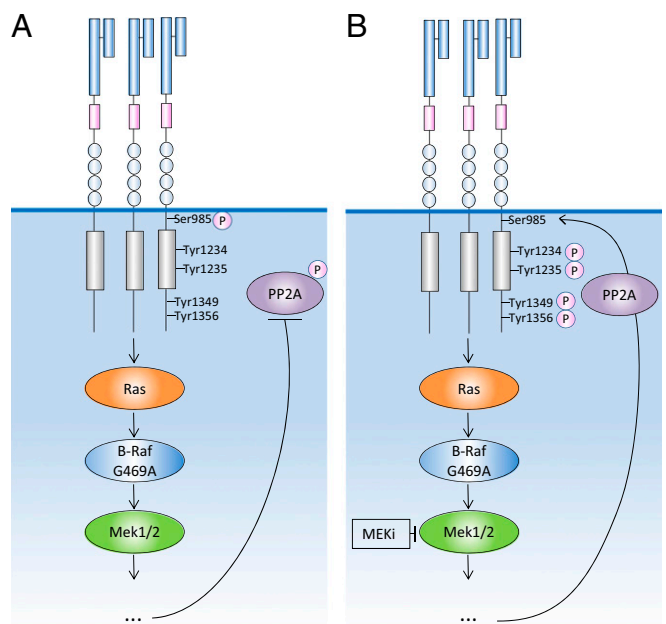

Fig. 5. Protein Phosphatase 2A (PP2A) welds a negative feedback loop between BRAF and MET. (*A*) In CUP liver metastatic cells featuring amplification of MET, the oncogenic kinase is silent. In these cells, mutation of BRAF, positioned in the MET downstream signaling cascade, inactivates PP2A, likely by tyrosine phosphorylation (37). In turn, the amplified MET receptor complex is inactivated by the known mechanism phosphorylating the inhibitory Ser985 (ref. 11, not shown in the scheme). (*B*) Blockade of the MEK unleashes PP2A activity, leading to dephosphorylation of the inhibitory Ser985. The MET receptor cluster is now reactivated and revives the transformed phenotype.

CELL BIOLOGY

mutated tumor with a MET inhibitor, as BRAF is downstream MET in the signal transduction cascade. On the contrary, these data provide a strong rationale for combinatorial therapy of MET-amplified/BRAF-mutated patients, who have poor clinical response to each inhibitor in monotherapy.

Materials and Methods

Tumor Sample. Informed consent for research use was obtained from the patient (ClinicalTrials.gov identifier: NCT03347318) at the enrolling institution FPO-IRCCS (Candiolo) before tissue banking, and study approval was obtained from the ethics committee of FPO-IRCCS (Candiolo).

Cell Cultures and Inhibitors. Primary cell line L1.13 was derived from PDX1.13. The tumor was explanted, digested with Collagenase I (Sigma-Aldrich), and cultured in RPMI medium 1640 (Sigma-Aldrich) supplemented with 10% serum (FBS; Sigma Aldrich). Cell genetic tumor identity has been identified by short tandem repeat profiling (Cell ID; Promega).

A549 were purchased from American Type Culture Collection, A2780 from European Collection of Authenticated Cell Cultures, and maintained in their original culturing conditions according to supplier guidelines.

AZD-6244 was purchased from Sequoia Research Products, TAK-632 from Selleck chemicals, NaF from Sigma Aldrich, and BEZ-652 from Selleck Chemicals, and JNJ-38877605 was kindly provided by Janssen Pharmaceutica NV.

siRNA. siRNA (Ambion) were transfected by Lipofectamine RNAiMAX (Invitrogen), according to manufacturer's instructions, and harvested 72 h after transfection.

PPP2CA Assay ID: s10958 (#58), s10959 (#59). Scrambled siRNA: Silencer Select Negative Control No. 1 siRNA.

Nucleic Acid Extraction. gDNA was extracted with Maxwell RSC Blood DNA Maxwell RSC Whole Blood DNA Kit (Promega), according to the manufacturer's protocol.

qRT-PCR. Gene copy number was performed by real-time PCR in triplicate on ABI PRISM 7900HT thermal cycler (Life Technologies), using Human TaqMan probes from Thermo Fisher Scientific: MET (assay ID Hs04993403_cn), EGFR (assay ID: Hs04942325_cn). RNase P was used as endogenous reference gene (TaqMan Copy Number Reference Assay, human, RNase P).

FISH Analysis. FISH analysis for the detection of MET gene copy number was performed on 5-μm paraffin-embedded tissue sections according to standard techniques. The tissue sections were incubated with the MET (7q31)/SE 7 dual-color probe (Kreatech; Leica Biosystems) and counterstained with DAPI I (Vysis-Abbott Molecular). The FISH analysis was performed with the fluorescence microscope BX61 (Olympus) and the automated FISH imaging platform Bioview (Abbott Molecular). An average of 100 nonoverlapping interphase nuclei with intact morphology was analyzed using H&E-stained sections as a hysto-topographic reference. MET gene was considered amplified when the MET/CEP 7 Ratio was ≥2 (44).

Mutational Analysis. gDNA was examined with OncoCarta Panel v1.0 (www.readcube.com/articles/10.1038/nmeth.f.254). Next-generation sequencing on 241 genes was performed using Illumina MiSeq. A custom pipeline was used for next-generation sequencing, to call somatic variations when supported by at least 1% allelic frequency and 5% Fisher's test significance level.

Flow-Cytometric Analysis. Cells (2×10^5) were incubated with the APC conjugated mouse anti-MET (FAB3582A, clone 95106; R&D Systems Inc.) and analyzed in a CyAn ADP 9 colors (Beckman Coulter). Data were analyzed using Summit 4.3 software (Beckman Coulter).

Western Blot, Immunoprecipitation, and Phosphokinase Array. Cells were lysed in EB buffer (50 mM Hepes at pH 7.4, 150 mM NaCl, 1% Triton X-100, 10% glycerol, 5 mM EDTA, and 2 mM EGTA) and resolved by SDS/PAGE as total lysates or immunoprecipitates. For immunoprecipitation, equal amounts of protein extract were immunoprecipitated using DO-24 antibody (45) adsorbed on Sepharose-protein G beads. Primary antibodies anti-MET (sc-10), anti-Actin (sc-1616), and P-PP2A (sc-271903) were from Santa Cruz Biotechnology; anti P-MET (Tyr1234/1235) (Clone D26), anti P-ERK (Thr202/Tyr204) (Clone D13.14.4E), anti-ERK, anti PP2A (catalog number #2038), anti P-AKT (Ser473; Clone D9E), and anti-AKT (Clone 40D4) were from Cell Signaling; anti-Vinculin (catalog number V9131) was from Sigma; and P-MET (Ser985) (catalog number PA5-64558) was from Thermo Fisher Scientific. Secondary antibodies were from Amersham.

The Phospho-Kinase Array Kits (Human Phospho-Receptor Tyrosine Kinase Array Kit, and Proteome Profiler Human Phospho-Kinase Array Kit; R&D Systems) were used according to the manufacturer's instructions.

In Vivo Experiments. PDX was obtained by s.c. implantation in the flank of a female NOD (nonobese diabetic) SCID mouse, 5 wk old, purchased from Charles River Laboratories. Tumors were then passaged until production of a cohort of 36 mice. Once tumors were established (average volume, 250/300 mm³), mice were randomized and divided into four cohorts (6 mice/cohort) and treated daily by gavage with vehicle, AZD-6244 (25 mg/kg), JNJ-38877605 (50 mg/kg), and a combination of the two drugs. Tumor size was evaluated weekly. All animal procedures were approved by the Italian Ministry of Health and the internal Ethical Committee for Animal Experimentation of Candiolo Cancer Institute, FPO-IRCCS.

Immunofluorescence and Immunohistochemistry. Twenty-four hours before death, mice were intraperitoneally injected with 75 μg/mouse EdU. Immunofluorescence was carried out on formalin-fixed paraffin-embedded (FFPE) tissues. Slides were stained using the Click-iT EdU AlexaFluor 555 Imaging Kit (Life Technologies), following the manufacturer's instructions, and with DAPI. At least 15 images have been acquired for each treatment group. Quantitative analyses of colocalization were carried out with ImageJ software (https://imagej.nih.gov/ij/).

Immunohistochemistry was carried out on FFPE tissues. Slides were incubated with the primary antibodies: P-ERK1/2 rabbit mAb (Thr202/Tyr204, clone D13.14.4E; Cell Signaling Technology) and P-MET (Tyr1234/1235) AF2480 from R&D Systems. Anti-rabbit secondary antibody (Dako Envision + System-horseradish peroxidase–labeled polymer, Dako) has been used. Immunoreactivities were revealed by incubation in DAB chromogen (DakoCytomation Liquid DAB Substrate Chromogen System; Dako). Slides were counterstained in Mayer's hematoxylin. A negative control slide was processed with secondary antibody without primary antibody incubation. Images were captured with 40× objective, and representative images were been acquired.

Statistical Analysis. Statistical analyses were performed by two-tailed Student's *t* test and two-way ANOVA, using the GraphPad Prism software. All experiments, except the in vivo trials and phosphokinase array analysis, were repeated at least three times. Figures show one representative experiment, reporting the average of the technical replicates. Statistical significance: $**P < 0.01$; $***P < 0.001$; $****P < 0.0001$.

1. Merlo LM, Pepper JW, Reid BJ, Maley CC (2006) Cancer as an evolutionary and ecological process. *Nat Rev Cancer* 6:924–935.
2. Hanahan D, Weinberg RA (2011) Hallmarks of cancer: The next generation. *Cell* 144:646–674.
3. Holohan C, Van Schaeybroeck S, Longley DB, Johnston PG (2013) Cancer drug resistance: An evolving paradigm. *Nat Rev Cancer* 13:714–726.
4. Gherardi E, Birchmeier W, Birchmeier C, Vande Woude G (2012) Targeting MET in cancer: Rationale and progress. *Nat Rev Cancer* 12:89–103.
5. Comoglio PM, Giordano S, Trusolino L (2008) Drug development of MET inhibitors: Targeting oncogene addiction and expedience. *Nat Rev Drug Discov* 7:504–516.
6. Stella GM, et al. (2011) MET mutations in cancers of unknown primary origin (CUPs). *Hum Mutat* 32:44–50.
7. Comoglio PM, Trusolino L, Boccaccio C (2018) Known and novel roles of the MET oncogene in cancer: A coherent approach to targeted therapy. *Nat Rev Cancer* 18:341–358.
8. Comoglio PM, Trusolino L (2002) Invasive growth: From development to metastasis. *J Clin Invest* 109:857–862.

9. Barrow-McGee R, Kermorgant S (2014) Met endosomal signalling: In the right place, at the right time. *Int J Biochem Cell Biol* 49:69–74.
10. Peschard P, et al. (2001) Mutation of the c-Cbl TKB domain binding site on the Met receptor tyrosine kinase converts it into a transforming protein. *Mol Cell* 8:995–1004.
11. Gandino L, Longati P, Medico E, Prat M, Comoglio PM (1994) Phosphorylation of serine 985 negatively regulates the hepatocyte growth factor receptor kinase. *J Biol Chem* 269:1815–1820.
12. McDermott U, et al. (2007) Identification of genotype-correlated sensitivity to selective kinase inhibitors by using high-throughput tumor cell line profiling. *Proc Natl Acad Sci USA* 104:19936–19941.
13. Bardelli A, et al. (2013) Amplification of the MET receptor drives resistance to anti-EGFR therapies in colorectal cancer. *Cancer Discov* 3:658–673.
14. Qi J, et al. (2011) Multiple mutations and bypass mechanisms can contribute to development of acquired resistance to MET inhibitors. *Cancer Res* 71:1081–1091.
15. Cepero V, et al. (2010) MET and KRAS gene amplification mediates acquired resistance to MET tyrosine kinase inhibitors. *Cancer Res* 70:7580–7590.
16. Marais R, Marshall CJ (1996) Control of the ERK MAP kinase cascade by Ras and Raf. *Cancer Surv* 27:101–125.
17. Davies H, et al. (2002) Mutations of the BRAF gene in human cancer. *Nature* 417:949–954.
18. Wan PT, et al.; Cancer Genome Project (2004) Mechanism of activation of the RAF-ERK signaling pathway by oncogenic mutations of B-RAF. *Cell* 116:855–867.
19. Forbes SA, et al. (2011) COSMIC: Mining complete cancer genomes in the catalogue of somatic mutations in cancer. *Nucleic Acids Res* 39:D945–D950.
20. Tsai J, et al. (2008) Discovery of a selective inhibitor of oncogenic B-Raf kinase with potent antimelanoma activity. *Proc Natl Acad Sci USA* 105:3041–3046.
21. Holderfield M, Deuker MM, McCormick F, McMahon M (2014) Targeting RAF kinases for cancer therapy: BRAF-mutated melanoma and beyond. *Nat Rev Cancer* 14:455–467.
22. Tirosh I, et al. (2016) Dissecting the multicellular ecosystem of metastatic melanoma by single-cell RNA-seq. *Science* 352:189–196.
23. Oddo D, et al. (2017) Emergence of MET hyper-amplification at progression to MET and BRAF inhibition in colorectal cancer. *Br J Cancer* 117:347–352.
24. Pietrantonio F, et al. (2016) MET-driven resistance to dual EGFR and BRAF blockade may Be overcome by switching from EGFR to MET inhibition in BRAF-mutated colorectal cancer. *Cancer Discov* 6:963–971.
25. Catalanotti F, et al. (2013) Phase II trial of MEK inhibitor selumetinib (AZD6244, ARRY-142886) in patients with BRAFV600E/K-mutated melanoma. *Clin Cancer Res* 19:2257–2264.
26. Ascierto PA, et al. (2013) MEK162 for patients with advanced melanoma harbouring NRAS or Val600 BRAF mutations: A non-randomised, open-label phase 2 study. *Lancet Oncol* 14:249–256.
27. Flaherty KT, et al. (2012) Combined BRAF and MEK inhibition in melanoma with BRAF V600 mutations. *N Engl J Med* 367:1694–1703.
28. Trusolino L, Bertotti A, Comoglio PM (2010) MET signalling: Principles and functions in development, organ regeneration and cancer. *Nat Rev Mol Cell Biol* 11:834–848.
29. Berns K, et al. (2007) A functional genetic approach identifies the PI3K pathway as a major determinant of trastuzumab resistance in breast cancer. *Cancer Cell* 12:395–402.
30. Nagata Y, et al. (2004) PTEN activation contributes to tumor inhibition by trastuzumab, and loss of PTEN predicts trastuzumab resistance in patients. *Cancer Cell* 6:117–127.
31. Manzano JL, et al. (2016) Resistant mechanisms to BRAF inhibitors in melanoma. *Ann Transl Med* 4:237.
32. Yeh TC, et al. (2007) Biological characterization of ARRY-142886 (AZD6244), a potent, highly selective mitogen-activated protein kinase kinase 1/2 inhibitor. *Clin Cancer Res* 13:1576–1583.
33. Okaniwa M, et al. (2013) Discovery of a selective kinase inhibitor (TAK-632) targeting pan-RAF inhibition: Design, synthesis, and biological evaluation of C-7-substituted 1,3-benzothiazole derivatives. *J Med Chem* 56:6478–6494.
34. Prahallad A, et al. (2012) Unresponsiveness of colon cancer to BRAF(V600E) inhibition through feedback activation of EGFR. *Nature* 483:100–103.
35. Shenolikar S, Nairn AC (1991) Protein phosphatases: Recent progress. *Adv Second Messenger Phosphoprotein Res* 23:1–121.
36. Hashigasako A, Machide M, Nakamura T, Matsumoto K, Nakamura T (2004) Bi-directional regulation of Ser-985 phosphorylation of c-met via protein kinase C and protein phosphatase 2A involves c-Met activation and cellular responsiveness to hepatocyte growth factor. *J Biol Chem* 279:26445–26452.
37. Chen J, Martin BL, Brautigan DL (1992) Regulation of protein serine-threonine phosphatase type-2A by tyrosine phosphorylation. *Science* 257:1261–1264.
38. Kim JY, et al. (2016) Phosphoproteomics reveals MAPK inhibitors enhance MET- and EGFR-driven AKT signaling in KRAS-mutant lung cancer. *Mol Cancer Res* 14:1019–1029.
39. Ponzetto C, et al. (1994) A multifunctional docking site mediates signaling and transformation by the hepatocyte growth factor/scatter factor receptor family. *Cell* 77:261–271.
40. Won JK, et al. (2012) The crossregulation between ERK and PI3K signaling pathways determines the tumoricidal efficacy of MEK inhibitor. *J Mol Cell Biol* 4:153–163.
41. Aparicio S, Caldas C (2013) The implications of clonal genome evolution for cancer medicine. *N Engl J Med* 368:842–851.
42. Tabassum DP, Polyak K (2015) Tumorigenesis: It takes a village. *Nat Rev Cancer* 15:473–483.
43. Ostman A, Hellberg C, Böhmer FD (2006) Protein-tyrosine phosphatases and cancer. *Nat Rev Cancer* 6:307–320.
44. Jurmeister P, et al. (2015) Parallel screening for ALK, MET and ROS1 alterations in non-small cell lung cancer with implications for daily routine testing. *Lung Cancer* 87:122–129.
45. Prat M, Crepaldi T, Pennacchietti S, Bussolino F, Comoglio PM (1998) Agonistic monoclonal antibodies against the Met receptor dissect the biological responses to HGF. *J Cell Sci* 111:237–247.

CELL BIOLOGY